Journal of Environment and Earth Science
ISSN 2224-3216 (Paper) ISSN 2225-0948 (Online)
Vol.13, No.2, 2023

Geochemistry and Petrology of Metasediments Associated with Gold Mineralization in Imonga Area, Eastern DR Congo

Mupenge M. Parfait[1,2]*, Sicke Lunkomo[1,3], Bishikwabo K. Germain[2], Raha Mulumba[1], Elia Mukingi B.[2], Daniel Akuzwe[2]
1. Department of Geology, Université Libre de Grands Lacs, Bukavu, DR Congo, E-mail: ulgl1@yahoo.fr
2. Department of Geology, Université Officielle de Bukavu, UOB, 570 Bukavu, DR Congo
3. Department of Geology, Université du Moyen Lualaba, Lualaba, DR Congo, Postal Code 136 Kalima
Corresponding author: parfaitmupenge@gmail.com

Acknowledgements
The Authors are grateful to SGS Twangiza DRC for providing the necessary laboratory facilities for samples analyses to this research of the Second Author. This paper is a part of the second author research; therefore, the authors thank Mr. Yogolelo Mukokya for his contribution during the review of the Second author's research from where this paper has been developed. In expansion, the Authors are without a doubt thankful of the meticulous survey and strong commitments of the nameless reviewers to the ultimate article.

Declaration
The authors declare that they have no known competing financial interests or personal relationships that could have appeared to influence the work reported in this paper.

Abstract
The Imonga sector is located in the Eastern of DR Congo, precisely within the Maniema province located in the Central African Karagwe Ankole belt, which forms together with the Kibara belt a Mesoproterozoic geological structure. This study gives fresh information on the origin of the metasediments in this zone, their geochemical and petrographic characteristics, and the genetic model of the gold mineralization that they contain. Field observations, as well as petrographic and geochemical studies reveal that the metasediments consist of sericitoschists and quartzites. Petrographic work revealed varying proportions of sericite and quartz with subordinate iron-oxide minerals. Geochemically, most of the analyzed metasediments displayed higher SiO_2 contents and enriched in Fe_2O_3. They belong to the groups of shales and sand (sometimes rich in iron), litharenite and grauwakes derived from quartzose sedimentary and mafic igneous provenance. Their protholites are intermediate altered ($70 < CIA < 90$) andesitic, granite and granodioritic rocks emplaced in a geotectonic active continental margin. Gold mineralization in the Imonga sector occur in veins. Gold mineralization is controlled by veins which occur as micro veins with small thickness. The mineralization consists of specific grains and nanoparticles pyrite associated with gold, hematite and goethite. The hydrothermal alteration accompanying this mineralization consists of silica, goethite and sericite-carbonate.

Keywords: Metasediment, sericitoschist, quartzite, sericite, goethite, vein, Gold, Imonga, Eastern DR Congo
DOI: 10.7176/JEES/13-2-04
Publication date: March 31st 2023

Introduction and general background

The province of Maniema in the east-central part of the Democratic Republic of the Congo is known for its numerous mineral deposits and deposits associated with the Kivaria chain. These are the Karimastin tungsten deposit previously developed by SOMINKI from 1776 to 1996, the Namoya gold deposit developed by Namoya Mining SA since 2015, and the Kabotshome gold deposit developed by Erongo Energy Ltd. Investigated in PR 4804 between 2011 and 2012. These various deposits are hosted in a world-class metallogenic chain known as the 'Twangiza-Namoya Chain' (Banro, 2010). Located northeast of the Kabotshome project, our study of the Imonga region is one of Maniema's distinct mining areas. The area has been mined for gold during the colonial period and in the last decade he has been mined by artisanal miners on six hills (Kanyabayonga, Kadiva, Mabanga, Nyungvira, Montbleu, Ngoko and Kabonga). rice field. Banro Congo Mining SA holds Exploration Permit 1552 in the area. According to Erongo Energy geologists (cited in Erongo Energy report, 2011, Sicke and Ombeni, 2017), the Kabatshome gold mineralization is permeated by the Kibaran-Mesoproterozoic-Metacediment. On the other hand, gold mineralization is found in the Paleoproterozoic Ruzisian metadediment of Mbutu Prospect. According to a technical report from Namoya Mining SA, a subsidiary of Banro Corporation, the mineralization of the Namoya deposit is controlled by his NW-SW oriented shear zones associated with the Paleoproterozoic Ruzizian chain (Banro, 2011 report). In addition, this mineralization is hosted by quartz and sulfide veins and by well-developed shaded metadediments. Namoya and Cabochome are still gold-producing areas in Maniema, but radiometric dating of Namoya and Cabochome gold mineralization has not been performed. In general, there are few large-scale geological studies of deposits in the Maniema area, mostly dating from the Belgian colonial period. (Varlamoff, 1948, 1950, 1954; 1956; De Kun, 1959; Steenstra, 1967). To date, no detailed geological survey of the Imonga

area and beyond has been conducted. The main geological data for the Imonga region of Maniema are based on interpretations of specific colonial regional geological maps (Cahen 1954; De Kun, 1959). The sector is shown to be composed of dolerite-interspersed metasediments (mica schist, black graphite schist and quartzite). Unpublished geological information about the area has revealed significant gold resources in the Imonga metasediment. This clearly indicates the need for additional research in this area, and the current study supports this view. Petrological and geochemical data of major and trace elements are used in this study to characterize the metadediment and mineralization of the Imonga sector. The nature, origin, geotectonic setting, and associated mineralization of metasediments are highlighted. Current research is primarily based on investigations of rock and metasediment samples collected during fieldwork.

Regional and Local geology

The Imonga area is located 210 km southeast of Kindu, capital of the Maniema province, and 130 km northeast of the town of Kasongo. Maniema province is located in the Central African Karagwe Ankole belt, which forms together with the Kibara belt a Mesoproterozoic geological structure (Tack et al., 2010). This structure extends from the southern part of the Katanga province in the Democratic Republic of Congo (DRCongo) to the southwestern part of Uganda (Fig. 1; Cahen et al., 1984). The two belts are separated by a Palaeoproterozoic basement rise that represents the NW extension across Lake Tanganyika of the Ubende belt (SW Tanzania). The geology of Maniema Province is characterized by Proterozoic formations and Phanerozoic coverages; the Proterozoic formations are divided into three: the Ruzizian (Paleoproterozoic), the Kibaran (Mesoproterozoic) and the Lindian (Neoproterozoic). The Phanerozoic formations include the sedimentary cover and the volcanic cover (Cahen, 1954). The characteristic Ruzizian formations outcrop in southern Maniema in the following sequence: Various phyllitic schists, quartzites, sericite schists, chlorite schists, amphibolitic schists and migmatitic gneisses (Le personne 1974). According to a recent report by Erongo Energie (2011) (cited in Sicke and Ombeni, 2017); during prospecting in Kasongo territory, Ruzizian age formations outcrop at Mbutu. The Ruzizian-age terrains are affected by basic magmatism characterized by green rocks whose nature and age are not yet known, but the acid magmatism that affects the Ruzizian-age terrains is characterized by granites, gneissic granites and migmatites(Lepersonne 1974). Lepersonne (1974) did not define a mineralization characteristic of the Ruzizian age terrains, but in the same report by the Erongo Energie Company, gold mineralization on the ground of formations considered to belong to the Ruzizian in this sector was highlighted. The Kibariene chain, currently referred to as the Kivu Supergroup, is generally oriented NE-SW in Kivu and NW-SE in Maniema. Lithostratigraphically, the Kivu Supergroup is subdivided into the following three groups The Nya-Ngezie Group younger than 1200Ma (Upper Kibaran) divided from top to bottom into the Mughera Formation, the Mukubio Formation and the Bangwe Formation. The Maniema Group (granite intruded at 1380Ma) that interests our work is subdivided into: The Mukombe formation of 600-800m is constituted of very hard meta-arkose with conchoidal fractures, massive texture and medium grains with siliceous cement. The Ngongomeka formation, with a thickness of 1000 to 1500m, is made up of black to dark grey or greenish-black metabasites that are cut in subhorizontal banks. The Lubile formation of 1000 to 1800m constitutes dark grey quartzite sandstone with alternating bluish-black and purplish-brown levels. The Bugarama Group (age greater than 1600Ma) is divided into the Mushenie Formation, Kamanyola Formation and Kashenie Formation. Structurally, the Kivu Supergroup, like the Karangwe-Ankole chain of southern Africa, is characterized by four deformation phases (Villeneuve, 1977; Theunissen, 1984; Klerkx et al, 1987; Rumvegeri, 1987; Pohl, 1987 and 1988): The first (D1) underlay the NE - SW oriented structures. It produced often isoclinal folds as well as foliation parallel to the layering, and was accompanied by syn-D1 metamorphism that is Barrow-like at Bunyakiri. The second phase (D2) is the paroxysmal phase; it is marked by NW - SE isoclinal folds. The syn-D2 metamorphism reached anatexis and led to the formation of granulites. The third phase (D2') corresponds to a late to post D2 shear episode. The structures it generates are sub-parallel to those given by D2. A fourth phase (D3) has been defined by Günther et al. (1989) and Pohl and Günther (1989, 1991), and has been related to acid magmatism bearing tin group mineralization.

From the magmatism point of view, the Kibaran chain is characterized by a bimodal magmatism (Rumvengeri, 1987; Talk et al., 2010; and Fernandez-Alonso et al. 2012). Two cycles of basic magmatism are reported in the Kibaran: Intercalary tholeiitic magmas in the Bugarama metasediments, and oceanic tholeiites of the Nya-Ngezi Group (Rumvegeri, 1987). Acid magmatism where four main acidic magmatic groups intruded the Kibaran formations (Cahen et al., 1984; Fernandez-Alonso et al., 1986; Pohl, 1987; Kanzira, 1989) (Fig.1): The G1 granite, intruded between 1325-1350 Ma (Ledent, 1979; Klerkx et al. 1984), consists of a biotite porphyritic and pre-D1 kinematic granite because it was deformed and mylonitized during the climax of this D1 deformation.

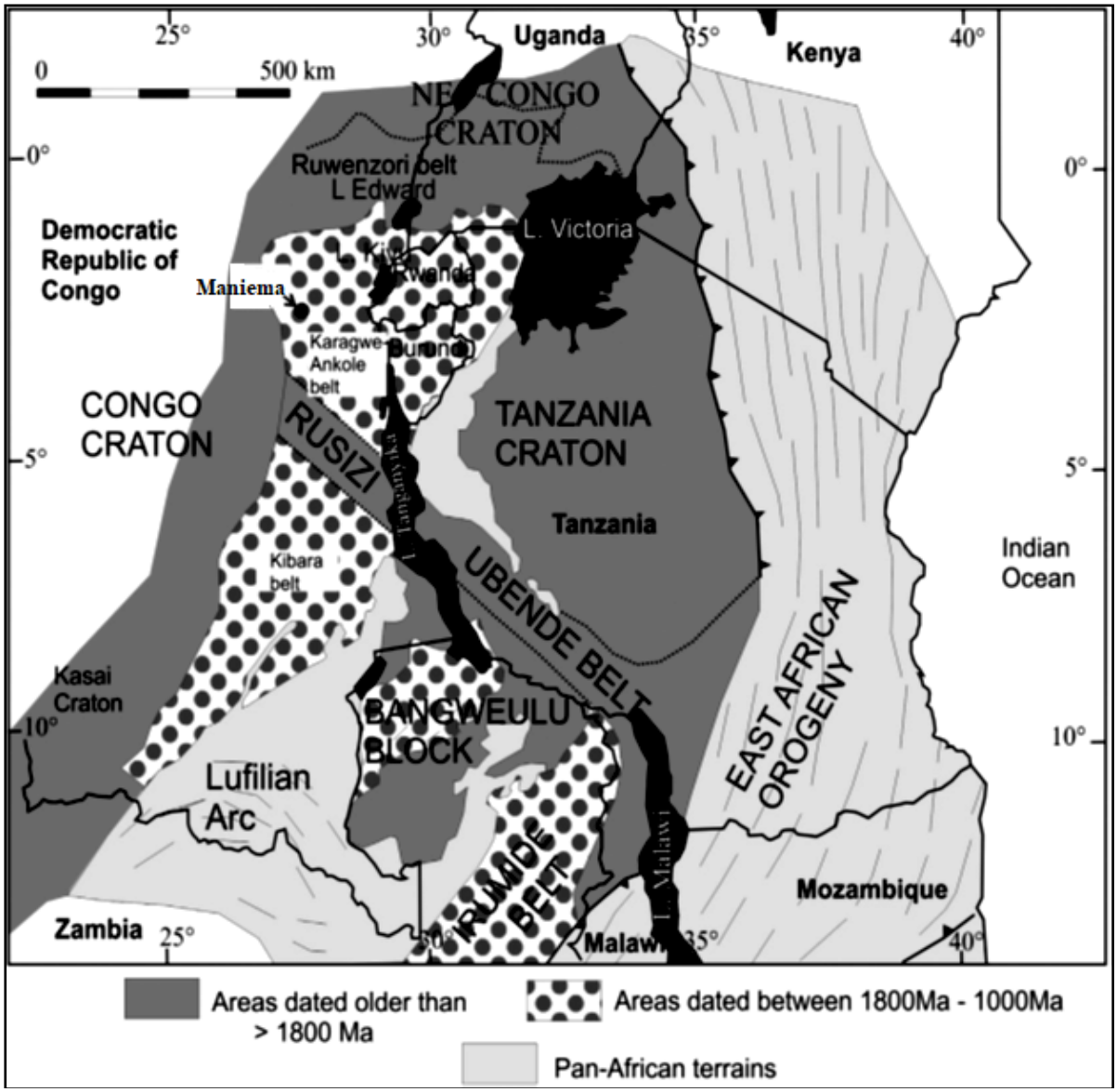

Fig. 1: Regional tectonic position of the Kibala Belt (KIB) and Karagwe-Angkor Belt (KAB) in Central Africa, showing the Maniema region (modified from Brinckmann et al., 2001).

Cahen et al.(1984) describe gneiss and porphyry adamerite with brown to greenish-brown biotite as the predominant mica. Its elongated minerals are friable and its microclinic crystals are generally granular. Plagioclase is often sericitized and its geochemistry shows alkali-calc affinity and superaluminum composition (Kanzira, 1989). G2 granite, syn-D2. Injected in the form of massifs consistent with the Nyangezi deposit (Fernandez-Alonso et al., 1986) is a biotite granite or two mica granites disproportionated by abundant xenoliths. Its emplacement is estimated at about 1200 Ma (Fernandez-Alonso et al., 1986). This type of granite was thought to be syn-D2. Tack et al. (1994) assigns ages over 1275 years. G3 granite, syn-D2'. Intruded between 1330–1260 Ma (Tack et al. 1994), it is composed of low-deformation 2-mica granites, sub-alkaline in composition, D'2 shear, synkinematic, complex basic and ultrabasic related to the body. G4 granites defined in Rwanda and Katanga (D.R.C.), Post Kibaran, Muscovite, and two rare micas. It is a small granite with an average age of 976 Ma (Cahen et al. 1984), which formed the last member of the Kibaran Magmatic Event and peaked between 1370 and 1310 Ma, composed of "special" sub-alkaline, post-orogenic muscovite (rarely 2 mica) and tourmaline-leuco granites. (Cahen et al. 1984). Its tectonothermal parin production coincided with the metal production peak of squirrel baran. Metallogenic data indicate that Kivu and Maniema Kibara are characterized by tin-group metal mineralization and gold mineralization in G4 (Cahen et al., 1984) and/or Gr5 (Tack et al., 2010) granites. However, some gold yields are unrelated to the G4 granite. Rather, they are of metamorphic origin (Braunschweig, 1992). Furthermore, Günther (1990) points out that the relationship between gold concentration and he G4 granite is speculative and highly questionable. Research is currently focused mainly on gold and metals associated with layered base intrusion, such as nickel, cobalt, copper, the platinum group, possibly titanium, vanadium and iron (Braunschweig, 1992).

Additionally, the chain appears to have excellent sources of industrial minerals (andalusite, feldspar, kaolin, muscovite, quartz, talc, wollastonite). Finally, there is evidence for metals associated with breath sediments (Braunschweig et al., 1992). Existing data on the study area from historical maps modified from Dekun (1959) showed that the local geology of the Imonga area is characterized by two majors geological lithologies, including shale and dolerite intrusions (Figure 2). The characteristic mineralization is gold mined from colluvial material or hosted in quartz veins intersecting shale and dolerite formations within the region.

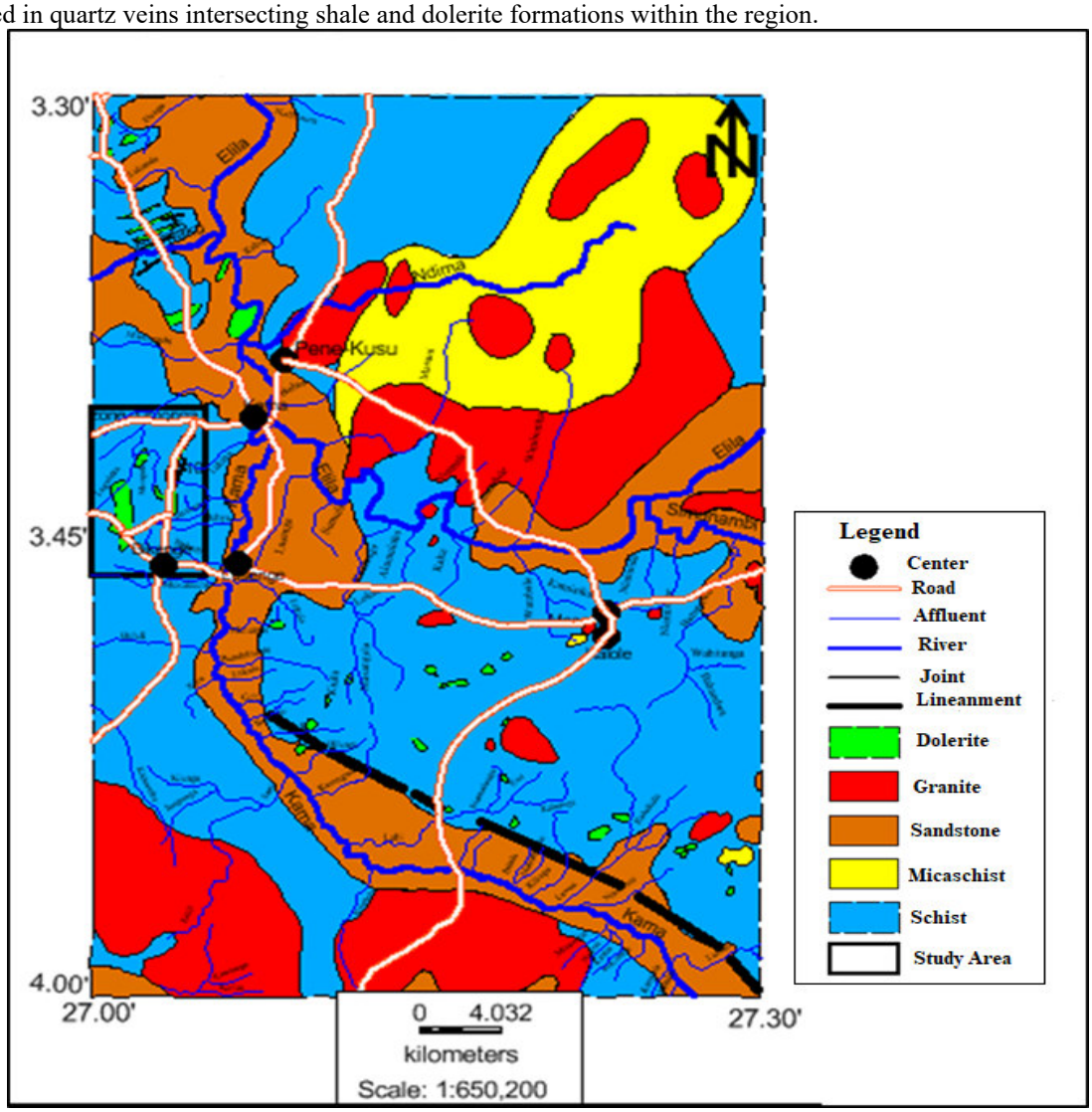

Figure 2: Geological of the zone showing the local geology of Imonga area modified after DeKun 1959.

Methodology

On the field, rocks were described in situ, and more than 20 samples of rocks were gathered for laboratory works. Thin sections and polished sections were made and the petrographic determinations were made at the Microsearch CC in South Africa. The petrographic study was carried out macroscopically and with the aid of a metallographic microscope outfitted with an image capture device linked to a computer. For geochemical analysis, 22 selected samples were dried in an electric oven at 100°C for less 4 to 6 hours to remove the water of imbibition, each sample was crushed in a jaw crusher to the nearest 0.5cm, then undergo the quartering (homogenization) to draw a part to be pulverized and each sample was pulverized to the nearest 75µm. Only 250gr of the pulverized sample was sent to the laboratory for their major, trace elements (As, Ba, Be, Bi, Cd, Co, Cr, Ni, Sb, Sn, Sr, V, W, Zr) and some metals compositions (Au, Mo, Cu, Zn, Pb, Ag) using XRF and ICP40B methods (SGS Tanzania Superintendence Co. Ltd.) and quantitative analyses have been done by the FAA505 fire assay (SGS-Twangiza, DR Congo) on selected samples to determine the gold content. For the analysis of gold and base metals, a blank sample, a duplicate sample and 4 standard samples were inserted according to the random that assigns each sample its number. The major and trace element concentrations of our samples were used by various diagrams through GcDkit software to determine the nature, provenance, and geotectonic environment of metasediments.

Results and discussions

Petrography

Although schists are totally altered (Fig. 3a) and not easy to find occur as outcrop within the area due the higher alteration degree, the metasediments are essentially composed of shists occur as sericitoschists and quartzites. The sericitoschists outcrop in almost the entire area while quartzite occurs as lens layers within some of the weathered sericitoschists in many places in the area. The sericitoschists are massive in appearance (Fig.3d, f) due to supergene alteration their original minerals and textures have been generally modified giving way to secondary minerals (sericite, chlorite, goethite, limonite and leucoxene) while quartzite rocks are moderately altered, massive and are composed macroscopically by quartz grains, iron oxides such as hematite, limonite, a large amount of sericite and sulfide can be identified disseminated within the rock (Fig.3b, c). The hydrothermal quartz veins contained in the meta-sediments, generally of a multi-centimeter thickness (Fig.3c), have a porphyritic texture. They consist of oxides, hematite and iron hydroxides (limonite), deposited within the quartz fragments (Fig. 3b, c and f). Generally, the metasediments are fine-grained, finger-staining, has a high degree of alteration, in gray in color and display iron oxide minerals such as hematite and limonite can be seen in diffuse form. Some sample rocks have voids (vuggs and boxwerks) left by oxidation of sulphide minerals (Fig. 4 a, b, c) while others present aligned minerals (Fig.5d) and massive form with fine granulometry (Fig.5e, q and q2). The microscopy investigations shown that the sericitoschist rocks display fine granulometry composed of the sericite the goethite, the limonite and the quartz. The sericite is evenly distributed and represents the average of 65.4% of the rock and is green, pale gray in color, fine grained, dominant as elongated palettes of size about 30µm and some grains reach 70µm, the goethite(opaque) and limonite represent 19.9% are xenomorphic with small size almost 30µm and irregularly distributed within the rock (Fig. 4a', b', c' and Fig. 5e', d') and could be formed during the process of oxidation and hydration or during the weak process of metamorphism. Quartz represents 1.2%, it is xenomorphic, white in color, less numerous related to goethite and limonite and is of size varying between 390µm to 1.21mm. While in quartzite, quartz is abundant 52.3% in average with remarkable rolling extinction and limonite and goethite found display average value of 32.8% of the total rock while muscovite is in less than 15% of the total rock and quartz veins can be identified within the rock microscopically (Fig.5q3 et q1).

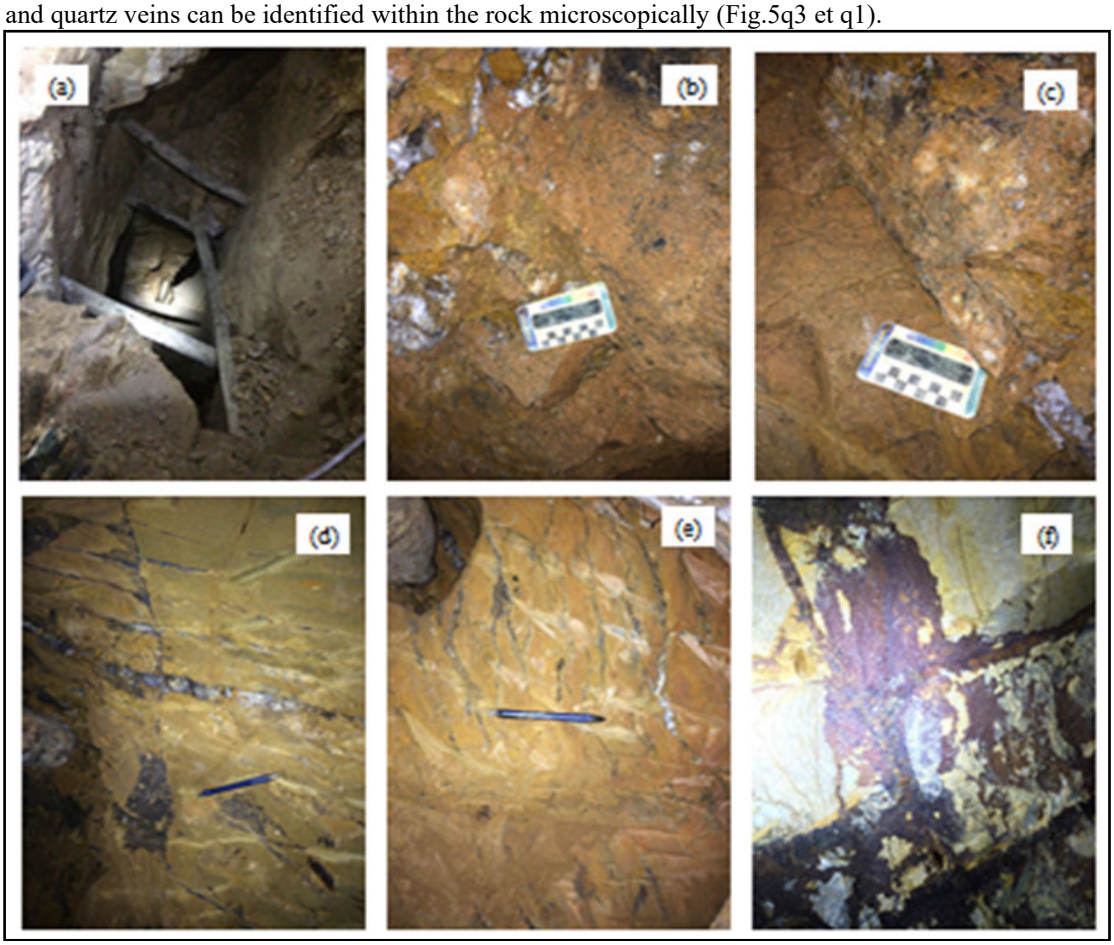

Fig.3: Photographs of the metasediments studied: (a) altered schist support open pit site. (b and c) altered quartzite cut crossing by micro and macro quartz veins, altered sericitoschist cut crossing by joints (d and e), and (f) altered sericitoschist rich in limonite cut crossing by micro quartz veins.

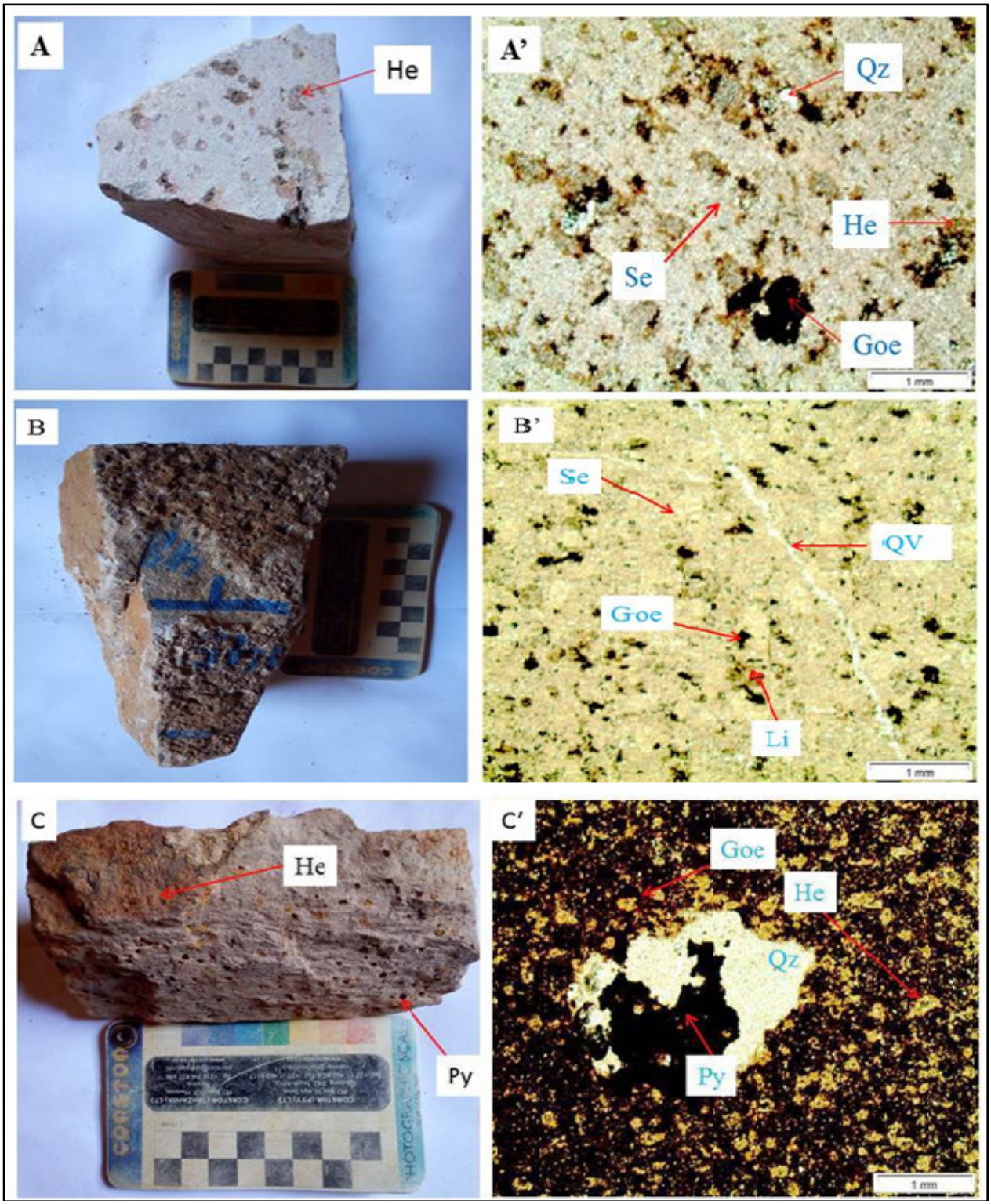

[He—hematite, Goe—Goethite, Li—limonite (oxides and hydroxides iron), Py—pyrite, Se—sericite, Qz—quartz].

Figure 4: Samples of metasediments from Imonga area (a,b,c) with their Microphotographs (a',b',c')

Figure 5: Samples of metasediments from Imonga area (D, E, Q2, Q) with their Microphotographs (D', E', Q3 and Q1)

Classification, chemical weathering, and compositional variation

The metasediments reveals a wide range for the major elements; they are siliceous (Table 1); with SiO_2 ranging from 64.12% to 75.63% (mean 71.76%), the TiO_2 ranges from 0.06% to 0.42% (mean 0.211%), the Al_2O_3 ranges from 3.34% to 15.94% (mean, 11.36%) while the range and mean content of other oxides in the metasediments

are as follows; Fe_2O_3 (3.27% to 21.16%, 8.44%), MgO (0.03% to 0.93%, 0.46%), CaO (0.02% to 0.30%, 0.06%), Na_2O (0.03% to 0.24%, 0.13%), K_2O (0.18% to 5.3%, 3.37%), P_2O_5 (0.07% to 0.41%, 0.18%) and MnO (0.01% to 0.9%, 0.11%). The range and average value of selected trace elements in the metasediments are as follows: As (122 - 42120 ppm, 1069.68ppm), Ba (520 - 2770 ppm, 1378.64), Be (0.5 – 2.3 ppm, 1.47), Sr (13.8 - 220 ppm, 72.23), Cd (1 - 23 ppm, 5.71), Sn (10 – 15ppm, 12.5), Cr(17 - 97 ppm, 58.09), Li (4 – 38 ppm, 19.45), V(72 - 600 ppm, 283.09), Zr (13.3 - 320 ppm, 118.99), Co (1 - 70 ppm, 15.81), Ni(4 - 56 ppm, 22.63), Sb (6 - 11 ppm, 8.125) and Sc (3.5 - 45 ppm, 20.31). The table shows La contents (7.4 - 191ppm, 61.18), Y (4.2 - 44 ppm, 19.9). In general, the metasediments shown important content for noble metals ranging respectively from (0.01 – 3.27ppm, average of 0.41) for Au, (11.6 – 260 ppm, average of 114.76) for Cu, (3– 81ppm, average of 25.09) for Mo, (16 – 320 ppm, average of 79.90) for Pb and (19– 240ppm, average of 64.40) for Zn. In other instances, the metasediments showed very little Bi, W, and Ag, displaying values below the detection threshold. According to the classification of Pettijohn et al. (1973), generally the investigated metasediments were plotted in the field of greywacke (Fig.6). This is corroborated the results on Fig.7 (Pettijohn, 1975) which show the only exception of one sample among all the analyzed samples in the field of arkose. The weathering history of igneous rocks has been considered by Fedo et al. (1995) using Al_2O_3 – (CaO+ Na_2O)–K_2O diagram. Na and Ca are taken out of the previously dissolved plagioclases during the early weathering stages. K-feldspar dissolves as weathering advances, releasing K instead of Al, causing the bulk composition trends of the residues to point toward the Al2O3 apex. Most samples lie in the clay mineral fields (Illite and muscovite trends), indicating an intermediate degree of weathering (Fig.8). Most of Investigated samples plot along the granite-rhyolite, granodiorite and andesite weathering trend, whereas few of them indicate high degree of weathering and displayed the fields of higher weathered clay minerals. Variation diagrams (Fig.9) show that Fe_2O_3, TiO_2, and Na_2O contents decrease with SiO_2, whereas K_2O and MgO contents increase with SiO_2. On the other hand, Cr, V, Ba, and Sr are positive correlated to Zr (Fig. 10), whereas Ni and As have a negative correlation with Zr. The investigated are relatively enriched in SiO_2, Fe_2O_3, Al_2O_3, K_2O, Ba, As, Cr, V, Ni, Sr, and Zr, but are depleted in Na_2O, CaO, MgO, TiO_2 and Be. K_2O/Na_2O is generally low in the metasediments with of an average value of 0.49 which is possibly a reflective of secondary addition of potassium (Table 2).

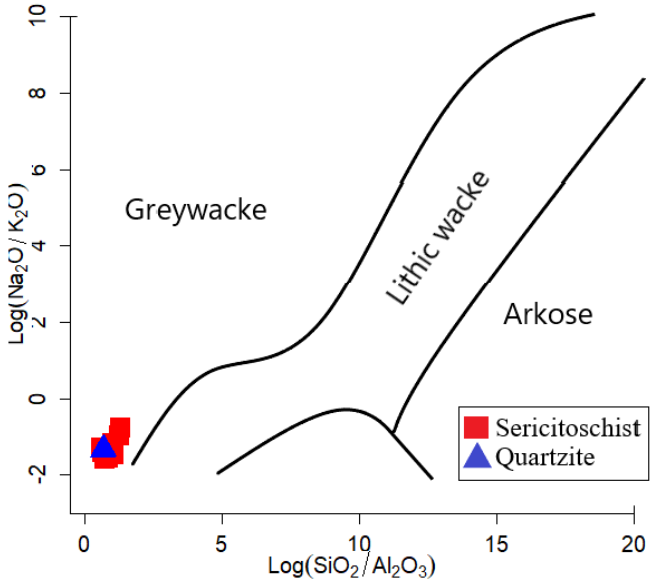

Fig.6: Classification log (Na2O/K2O) vs. log (SiO2/ Al2O3) discriminating diagram (after Pettijohn et al. 1973)

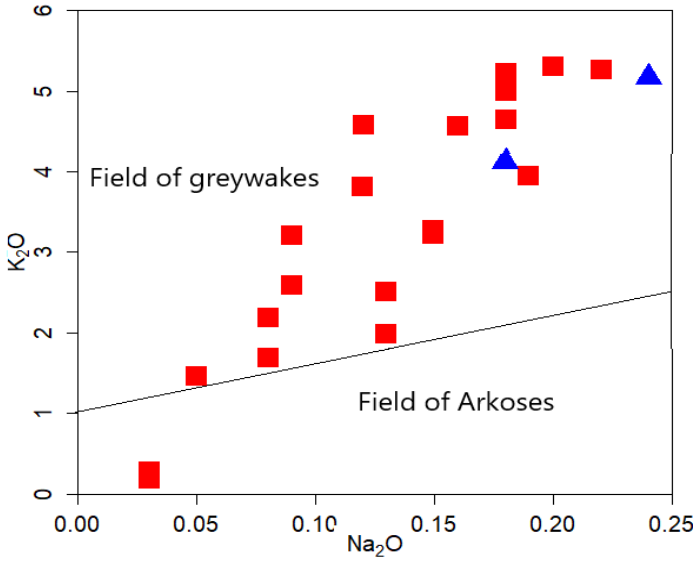

Figure 7: The plot of Na2O against K2O (Pettijohn, 1975)

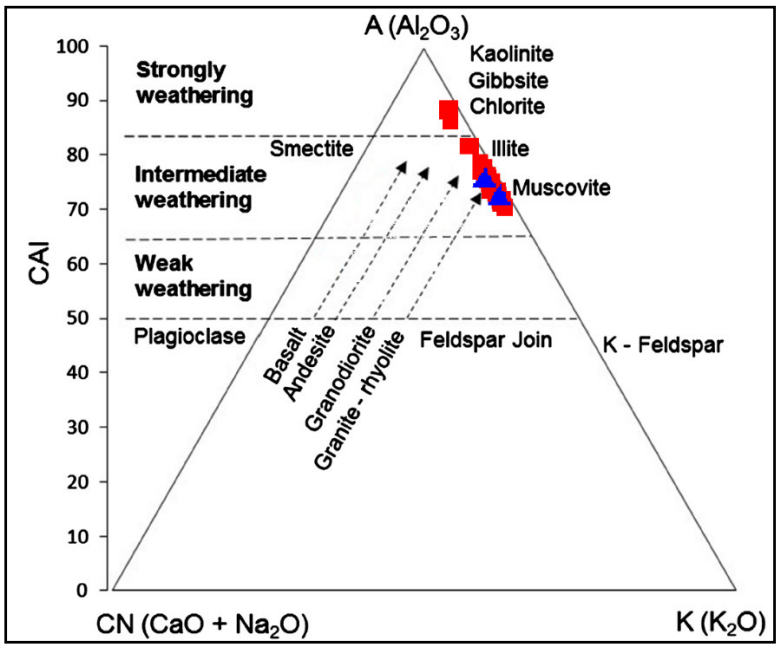

Figure 8: A-CN-K and CIA (Fedo et al. 1995)

The trace elemental content of metasedimentary rocks is influenced by a number of variables that may reflect different protolith formation processes (such as source composition, weathering, flow sorting), as well as diagenesis and metamorphism modifications (Fralick and Kronberg,1997) and the metasediments' varying trace element compositions may be a result of metamorphic processes, mineral fractionation during turbidity current deposition, or a combination of these (Condie et al. 1991). Geochemical analytical result reveals an enhancement of Ba which can be attributed to derivation from K-feldspar rich protolith; this is supported by the relatively high values of Ba. The relative enrichment of Ba coupled with the strong depletion of Sr relative to PAAS (Taylor and McLennan,1985, McLennan, S.M. 2001), NASC (Gromet et al., 1984), and UCC (Rudnick and Gao, S. 2003) is consistent with the general relative low abundance of CaO, implying that the source material of metasediments is plagioclase-poor. Ni, Sc, Cr and V are compatible ferromagnesium trace elements. In comparison to the UCC, which had values (in ppm) of 47, 92, 14, and 97 for Ni, Cr, Sc, and V, the NASC had values (in ppm) of 58, 125, 15, and 130 for Ni, Cr, Sc, and V, and the PAAS had values (in ppm) of 55, 110, 16, and 150 for Ni, Cr, Sc, and V; the metasediments in the study area are depleted in Ni, Cr with average values (in ppm) of 22,63 and 58,09 ppm respectively, in other hand there are riche with average value (in ppm) of 20,32 and 283,091ppm in V and Sc respectively (Table 2).

Sample No	975540	975541	975543	975549	975550	975552	975553	975554	975555	975556	975557	975566	975568	975569	975570	975571	975572	975573	975574	975585	LM009	LM010
	Sericitoschist																				Quartzite	
Major elements (%)																						
SiO2	69.87	72.41	75.52	75.05	73.92	71.42	75.63	75.35	66.72	74.99	72.31	75.30	71.36	68.25	67.24	64.12	68.89	66.53	75.62	71.67	71.60	74.99
TiO2	0.28	0.25	0.20	0.17	0.18	0.10	0.08	0.17	0.09	0.06	0.10	0.23	0.30	0.28	0.42	0.25	0.37	0.40	0.10	0.07	0.32	0.23
Al2O3	12.56	12.94	13.96	13.83	10.58	9.88	6.12	13.36	3.34	3.83	9.60	15.57	14.53	11.47	15.94	8.05	15.38	14.72	7.31	6.54	15.57	14.92
Fe2O3	6.99	3.27	6.54	6.59	10.24	5.48	4.08	4.12	4.26	8.25	16.45	4.59	9.45	13.84	21.16	5.01	10.83	14.73	9.11	9.21	7.46	4.10
MgO	0.93	0.63	0.63	0.71	0.55	0.46	0.23	0.73	0.03	0.07	0.36	0.75	0.61	0.40	0.25	0.27	0.32	0.28	0.23	0.12	0.91	0.71
MnO	0.17	0.01	0.01	0.01	0.01	0.01	0.01	0.01	0.02	0.02	0.05	0.06	0.09	0.11	0.80	0.90	0.15	0.01	0.03	0.08	0.05	0.00
CaO	0.12	0.05	0.07	0.05	0.05	0.02	0.02	0.05	0.02	0.05	0.07	0.05	0.05	0.07	0.07	0.07	0.07	0.05	0.10	0.05	0.30	0.05
K2O	4.58	4.65	4.57	4.99	3.81	3.21	1.46	5.23	0.18	0.28	2.59	5.30	5.27	3.27	2.51	2.19	3.95	3.22	1.69	1.99	4.12	5.17
Na2O	0.12	0.18	0.16	0.18	0.12	0.09	0.05	0.18	0.03	0.03	0.09	0.20	0.22	0.15	0.13	0.08	0.19	0.15	0.08	0.13	0.18	0.24
P2O5	0.21	0.14	0.32	0.14	0.23	0.11	0.07	0.11	0.09	0.21	0.37	0.07	0.09	0.18	0.27	0.16	0.23	0.21	0.41	0.07	0.23	0.07
TOT	95.83	94.53	101.98	101.71	99.68	90.79	87.75	99.30	74.78	87.79	102.00	102.12	101.97	98.02	108.80	81.09	100.37	100.28	94.69	89.92	100.73	100.50
Trace elements (ppm)																						
As	1020	280	940	1580	3070	1440	1220	920	940	1480	4120	122	360	380	460	191	740	620	2490	680	240	240
Ba	1440	1860	2770	1620	1440	1380	720	1860	520	1240	1360	1100	1120	800	880	1040	2400	1420	2040	540	1660	1120
Be	2.2	0.8	1.8	2.1	1.8	1.5	0.6	1.5	0.5	1	2.3	1.2	<0.5	<0.5	<0.5	<0.5	<0.5	<0.5	2.1	0.7	2.1	1.4
Bi	<5	<5	<5	<5	<5	<5	<5	<5	<5	<5	<5	<5	<5	<5	<5	<5	<5	<5	<5	<5	<5	<5
Cd	4	1	5	8	16	7	6	4	4	8	23	<1	2	1	2	2	4	3	14	3	1	2
Co	70	<1	<1	<1	<1	<1	<1	<1	<1	3	6	1	6	10	7	11	27	19	<1	14	<1	<1
Cr	71	59	71	87	68	53	22	55	17	18	57	85	87	55	29	38	63	82	46	44	97	74
Ni	31	8	15	6	7	7	9	9	20	34	50	12	27	39	25	12	53	56	25	33	16	4
Sb	<5	<5	10	7	7	7	<5	<5	<5	<5	<5	11	<5	<5	<5	<5	<5	6	7	<5	<5	10
Sn	<10	<10	<10	<10	10	<10	<10	<10	<10	<10	14	<10	<10	11	15	<10	13	12	<10	<10	<10	<10
Sr	99.2	72.1	188	40	38.9	56.2	48.5	114	26.8	85.5	182	37.6	30.9	13.8	18.6	97.5	78.9	33	220	35.9	47.1	24.7
V	220	420	340	420	300	280	125	320	72	87	320	460	460	340	600	123	165	220	198	93	520	145
W	<10	<10	<10	<10	<10	<10	<10	<10	<10	<10	<10	<10	<10	<10	<10	<10	<10	<10	<10	<10	<10	<10
Zr	157	119	118	100	91.6	75.8	43.1	125	13.3	26.1	87.8	81.3	200	108	73	137	88.8	320	220	133	123	177
La	60.3	80.6	79.2	53.7	39.9	41.2	25.6	55.9	7.4	9.9	39.2	14	87.7	77.1	41.1	38.7	191	144	98.6	35.4	43.9	81.6
Li	38	31	31	32	24	20	12	33	12	16	24	19	29	24	15	8	4	12	7	6	6	25
Sc	17.9	18.3	19.6	18.5	16.4	11.8	7	15.3	3.5	4.3	21.3	39.9	21.3	20.1	17.7	45	13.5	24.5	27.8	37.5	26.4	19.4
Y	44	23.2	31.1	14	16.7	12.3	7.5	19.5	4.2	7.2	22.5	27.2	21.1	17.3	17.8	15.5	17.4	37.2	24	19.9	13.2	25
Noble metals																						
Au	0.02	0.02	0.53	0.22	0.18	0.09	0.56	0.58	0.58	1.12	3.27	0.02	0.03	0.14	0.06	0.03	0.18	0.2	1.21	0.07	0.00	0.00
Ag	<2	<2	<2	<2	<2	<2	<2	<2	<2	<2	<2	<2	<2	<2	<2	<2	<2	<2	<2	<2	<2	<2
Cu	189	83.3	260	129	132	114	110	81.5	114	120	184	31.9	124	143	145	78	82.9	68.2	168	138	17.4	11.6
Mo	19	19	18	38	54	26	21	25	20	19	65	18	38	19	5	3	8	6	81	4	37	9
Pb	24	41	52	60	71	130	94	43	19	47	16	19	23	22	28	320	260	58	33	220	27	151
Zn	116	31	35	35	36	30	28	34	35	68	132	40	43	71	71	240	105	105	49	54	40	19

Table 1: Whole rock chemical composition of the studied metasediments

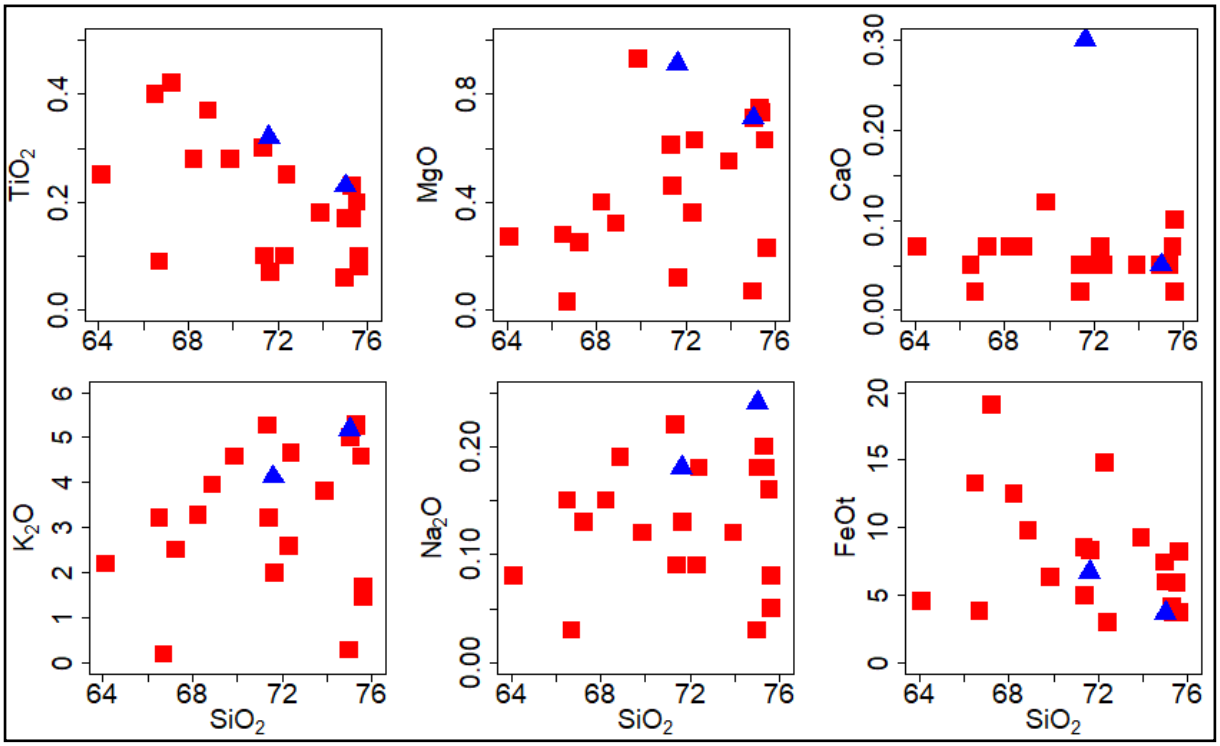

Fig. 9: SiO2 versus major elements variation diagrams for the investigated metasediments. Symbols as in Fig.1

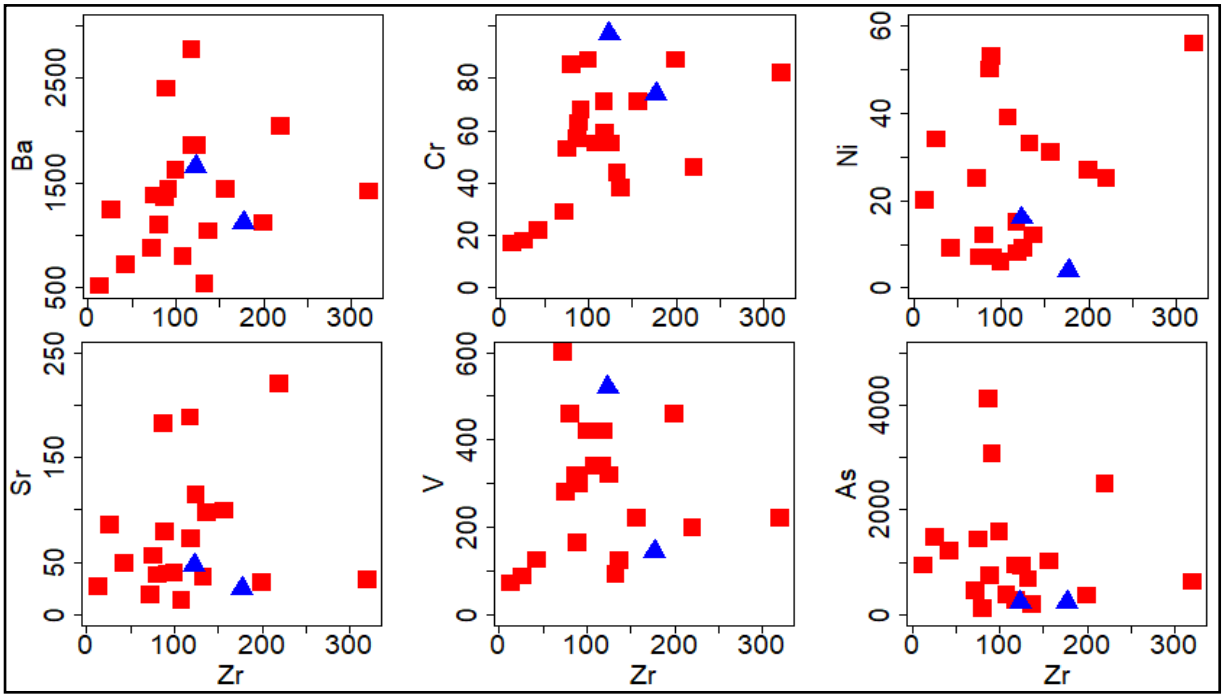

Fig. 10: Zr versus some selected trace elements variation diagrams for the investigated metasediments. Symbols as in Fig1

Table 2: Major elements of metasediments average, major and trace element compositions of studied metasediments in comparison to international references.

Reference	This study	PAAS	NASC	Upper Continental Crust (UCC)
SiO_2	71.76	62.80	64.80	66.60
TiO_2	0.21	1.00	0.70	0.64
Al_2O_3	11.36	18.90	16.90	15.40
Fe_2O_3	8.44	6.50	5.67	5.04
MgO	0.46	2.20	2.89	2.48
MnO	0.12	0.11	0.06	0.10
CaO	0.07	1.30	3.63	3.59
K2O	3.37	3.70	3.97	2.80
Na2O	0.14	1.20	1.14	3.27
P2O5	0.18	0.16	0.13	0.15
TOT	96.12	97.87	99.86	100.05
Ba	1,378.64	650.00	636.00	62.00
Cr	58.09	110.00	125.00	92.00
Ni	22.64	55.00	58.00	47.00
Sr	72.24	200.00	142.00	320.00
V	283.09	150.00	130.00	97.00
La	61.18	38.20	31.10	31.00
Sc	20.32	16.00	15.00	14.00
Y	19.90	27.00	35.00	21.00
K_2O/Na_2O	0.05	3.08	3.48	0.86
SiO_2/Al_2O_3	7.69	3.32	3.83	4.32
La/Sc	3.46	2.38	2.07	2.21
Zr/Sc	6.18	13.13	13.33	13.79

Tectonic setting and provenance

Various discriminating diagrams and ratios are used to evaluate the geodynamic deposition environment of the detrital sediments that led in the formation of the Imonga metasediments under. K_2O/Na_2O ratios reflect the active continental margin for the Imonga metasediments that is proved by the SiO_2 vs. Log (K_2O/Na_2O) tectonic discrimination diagrams after Roser and Korsh (1986) (Fig. 11), which is due to higher SiO_2 content and lower abundance of Na_2O and K_2O. Identical results are obtained on Fig.12 (Maynard et al., 1982; Roser and Korsch 1988),the investigate metasediments show active continental margin reflecting felsic source rocks which is confirmed by (Fig. 13) the TiO_2-K_2O-P_2O_5 ternary plot (after Pearce et al., 1975) of the metasediments in the study area. These immobile chemical components (SiO2 and TiO2) can reveal details about the origin and protholite composition of our samples. As a result, under the classification system for TiO_2 and SiO_2 (Tarney, 1977), the analyzed meta-sediments are rich in SiO_2 with varying concentrations of TiO_2 and are scattered within the field of sedimentary rocks mostly than the field of igneous rocks (Fig. 14). Floyd et al. (1989, 1991) used a plot to distinguish between primary (such as source regulated) and secondary (such as sedimentary reworking) controls on the composition of metasediments by employing the relatively immobile elements Ti and Ni in the metasediments. According to their graphic, the samples under investigation fall into two categories: sedimentary provenance and the compositional fields of immature and mature sediments regulated by magmatic antecedent rocks. The majority of the examined and analyzed metasediments exhibit acidic characteristics, and the relatively quit higher degree of scatter of the samples indicates that these metasediments were derived from mixed provenance source rocks (Fig.15). Using a categorization technique based on Log (Fe_2O_3/K_2O) vs Log SiO_2/Al_2O_3 after Herron (1988), the same findings are achieved (1988). The meta-sediments analyzed showed low SiO_2/Al_2O_3 and Fe_2O_3/K_2O ratios and would come from shales and sand (sometimes rich in iron), litharenite and grauwakes (Fig.16). Roser and Korsch (1988) identified four differing provenance groups: P1 (mafic), P2 (intermediate), P3 (felsic), and P4 (recycled). A function plot (Fig.17) shows that metasediments are plotted mainly within quartzose sedimentary provenances (recycled) and to some extent within mafic igneous provenance field. The higher SiO2 contents for the most of investigated metasediments implying a contribution of quartzose sedimentary source. V, Cr, Co, and Ni are compatible elements during igneous fractionation processes and are generally depleted in felsic rocks and enriched in mafic rocks. Variation diagrams (Fig.10) and Table 1 show some of the Imonga metasediments to be enriched in Fe_2O_3, V, Cr and Ni implying a contribution of mafic source of few of these

metasediments.

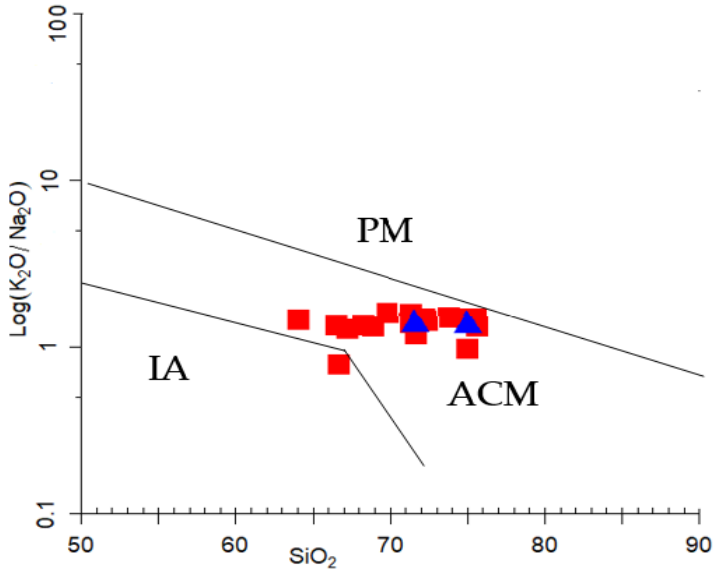

Fig. 11: SiO2 vs. K2O/Na2O Tectonic discrimination and source characteristics diagram (after Roser and Korsh 1986).

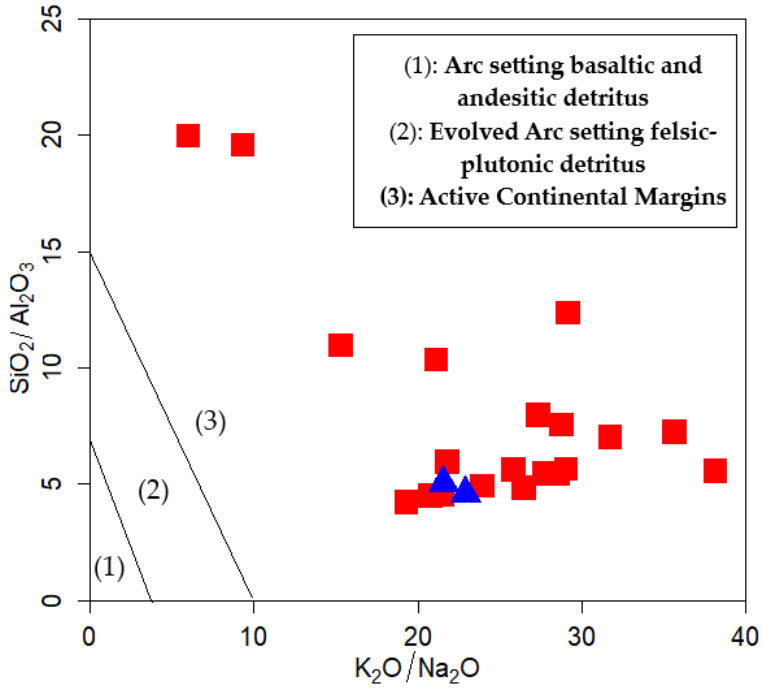

Fig.12: Tectonic discrimination diagrams and source characteristics diagram K2O/Na2O vs. SiO2/Al2O3 (Maynard et al. Roser and Korsch 1986).

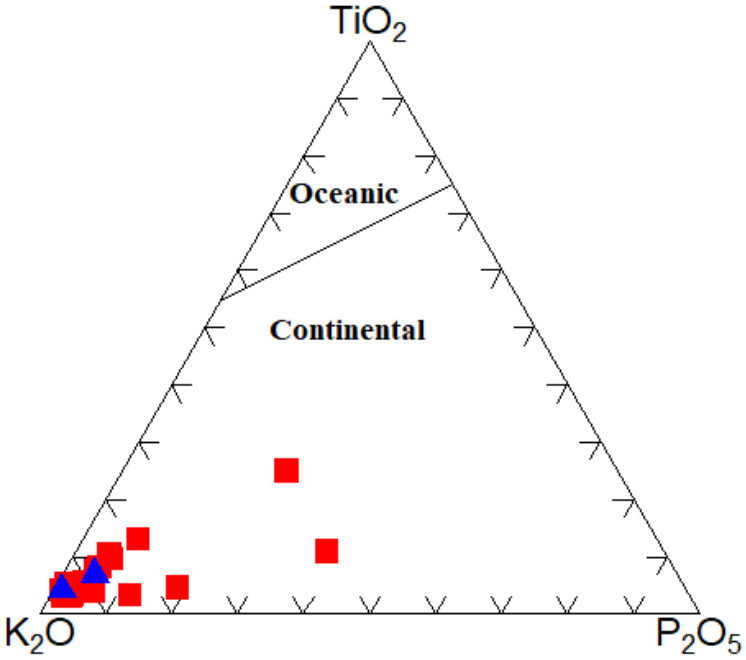

Fig. 13: TiO2-K2O-P2O5 ternary plot (after Pearce et al., 1975)

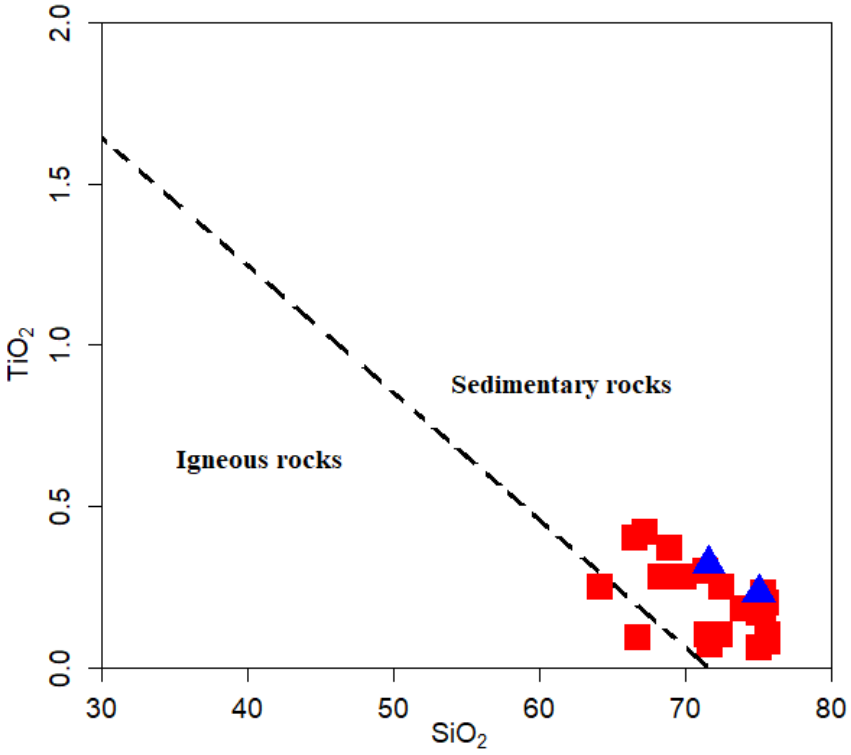

Fig. 14: Metasediments location in diagrams: (a) TiO2 versus SiO2 (Tarney, 1977)

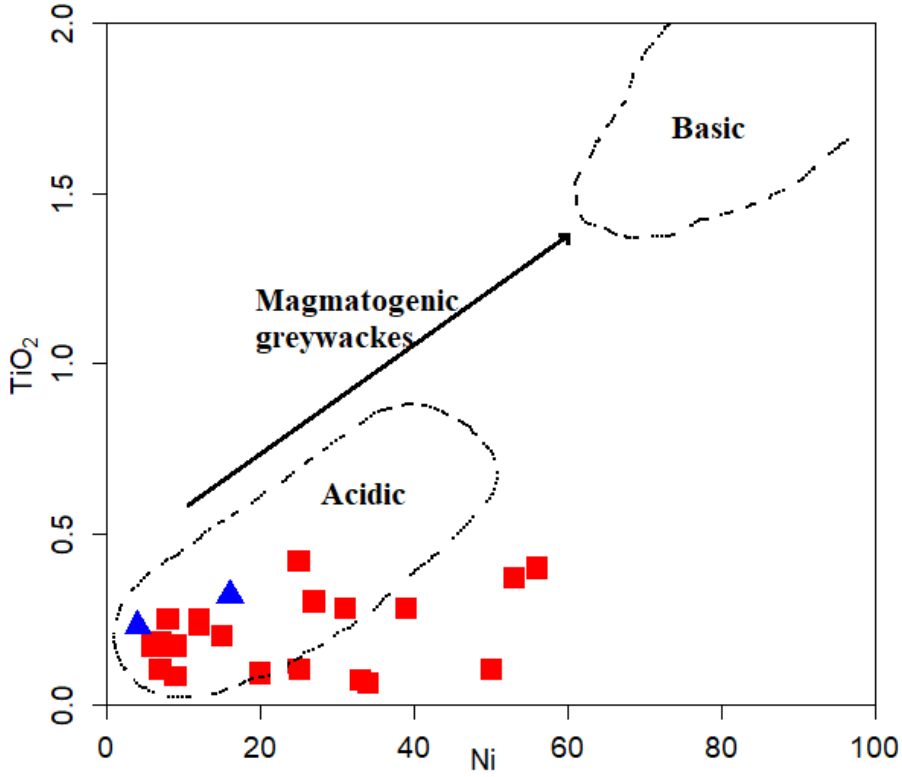

Figure 15: Ni vs, TiO2 plot (Floyed et al. 1989, 1991)

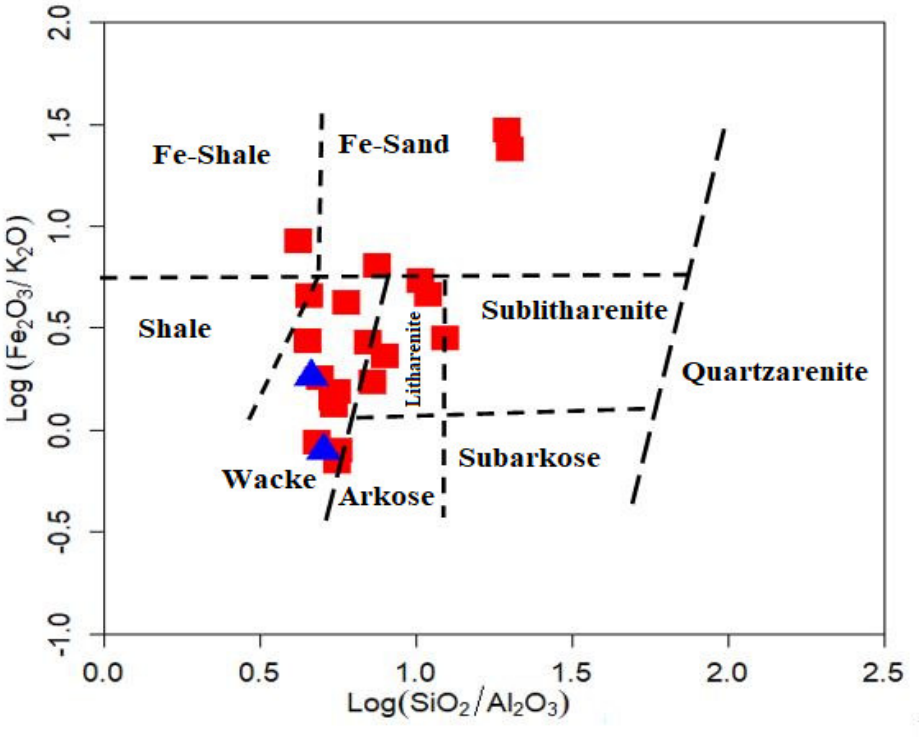

Fig.16: Log (Na2O/K2O) versus Log (SiO2/Al2O3) after Herron (1988)

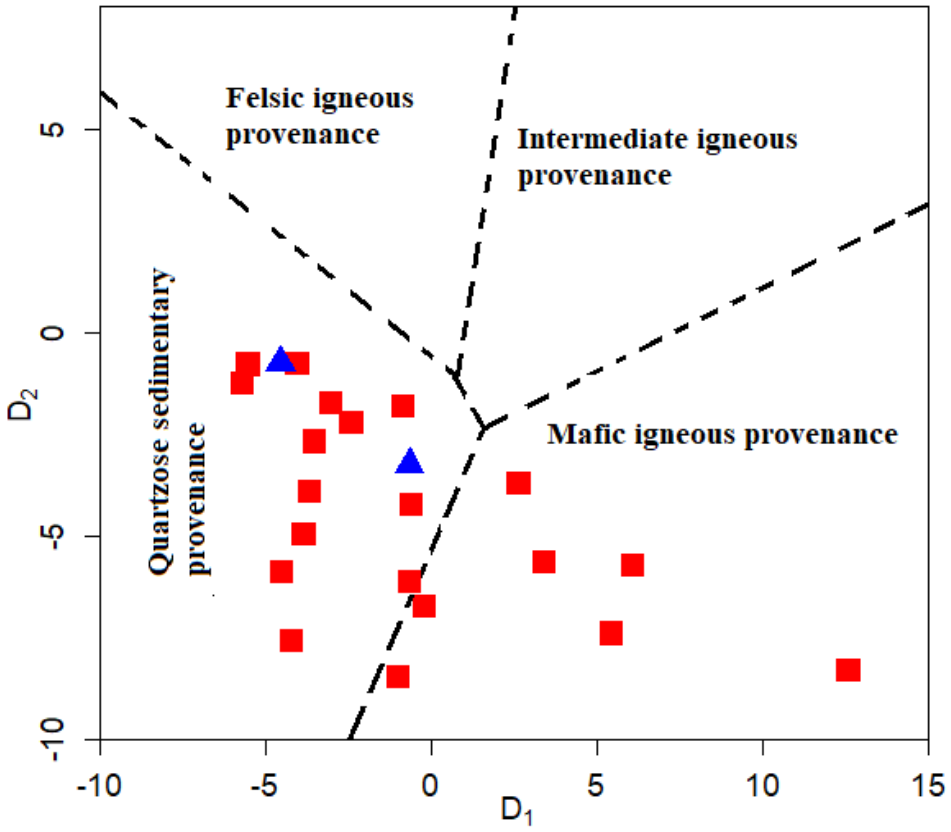

Figure 17: Discriminant function analysis classification plot (provenance fields after Roser and Korsch 1988).

Mineralization Associated with Imonga metasediments

Metasediments in the Imonga sector have been affected by metamorphic and tectono-sedimentary fluid that has disseminated as veins (Fig.3b and c). Due to the movement of hydrothermal fluids that cause neoformations, these various veins are typically recrystallized in silica, carbonates, micas, sulphides, oxides, with a lesser extent, arsenopyrite and precious metals. Gold mineralization occurs in a context of polyphase (ductile-brittle and brittle) tectonic deformation marked by NW-SE and NNE-SSW shears. According to Sibson and Scott (1998) the "fault-valve" concept given by, the genetic mineralization model that is typically accepted in such a geological environment is that of a continuum of fluid flows from ductile phases to brittle stages in relation to the initiation of earthquakes. In fact, every time the fluid pressure surpasses the lithostatic pressure, the resulting rock fracturing creates drains that allow hydrothermal fluids to circulate, creating the mineralized zones (Sibson et al., 1988). With a decrease in pressure, these fluids precipitate their mineral content, thus filling the veins. Although gold is the only mineral mined in this area, geochemical data show significant indicators of Mo, Cu, Pb and Zn content with mean values (in ppm) of ppm, respectively. 25.09, 114.76, 79.90 and 64.40.

Conclusion

Imonga metasediments in the Eastern DR Congo area consist of sericitoschists and quartzites, sericitoschists are most abundant that quartzite. The occurrence quartzite as layers within some of the weathered sericitoschists is evidence of sediment deposition under unstable flow regimes with both heavy and light sediments deposited. Petrographic investigations shown the enrichment in sericite, goethite, limonite, hematite respectively according to the degree of abundance. Geochemical data suggest that the metasediments from Imonga area are acidic due to due to higher SiO_2 content and would come from shales and sand (sometimes rich in iron), litharenite and grauwakes. These rocks would be emplaced in a tectonic environment of active continental margin. These metasediments were derived from mixed provenance source rocks, the higher SiO_2 contents for the most of investigated metasediments implying a contribution of quartzose sedimentary source while the enrichment in Fe_2O_3, V, Cr and Ni indicate a contribution of mafic source of few of these metasediments. Gold mineralization is controlled by veins which occur as micro veins with small thickness. The mineralization consists of specific grains and nanoparticles pyrite associated with gold, hematite and goethite. The hydrothermal alteration accompanying this gold mineralization consists of silica and sericite carbonates.

References

Banro Congo Mining, Rapport mensuel, septembre et Octobre (2010).
Banro Congo Mining, Rapport mensuel, septembre et Octobre (2011).
Braunschweig, T. (1992). Métallogénie de la Chaîne Kibarienne - Afrique Centrale. Ed. MRAC, 1992, 156p.
Brinckmann, J., Lehmann, B., Hein, U., Hohndorf, A., Mussallam, K., Weiser, Th, and Timm, F., (2001). La géologie et la minéralisation primaire de l'or de la chaîne Kibarienne, Nord-Ouest du Burundi, Afrique orientale. Geol. Jahrb. Reihe D. 101, 195.
Cahen, L. (1954). Géologie du Congo Belge, H. Vaillant-Carmann, Liège, Belg. 570p.
Cahen, L., Snelling, N.J., Delhal, J., Vail, J.R., Bonhomme, M., Ledent, D., (1984). The Geochronology and Evolution of Africa. 512 p. Clarendon Press, London.
De Kun, N. (1959). Les gisements de Cassitérite et de Columbo-tantalite du Nord Lugulu, Kivu, Congo Belge. Ann. Soc. Géologique de Belgique T. LXXXII, Mémoires 1959-1960
Fedo, C.M., Nesbitt, H.M., Young, G.M.,(1995). Unraveling the effects of potassium metasomatism in sedimentary rocks and paleosols, with implications for paleoweathering conditions and provenance. Geology 23, 921–924.
Fernandez-Alonso, M., Lavreau, J., Klerkx, J. (1986) Geochemistry and geochronology of the Kibaran granites in Burundi, Central Africa: Implications for the Kibaran orogeny, pp. 217-234.
Fernanadez-Alonso, M., Cutten, H., De Waele, B., Tack, L., Tahon, A., Baudet, D., Barritt, S.D., (2012). The Mesoproterozoic Karagwe-Ankole Belt (formerly the NE Kibara belt): The result of the prolonged extensional intracratonic basin development punctuated by two short-lived far -field compressional events. Precambrian Res. 63–86.
Floyed PA, Winchester JA, Park RG (1989) Geochemistry and tectonic setting of Lewisian clastic metasediments from the early Proterozoic Loch Maree Group of Gairloch, NW Scotland. Precam Res 45:203– 214
Floyed, P. A., Shail, R., Leveridge, B. E. and Franke, W. (1991). Geochemistry and provenance of Rhenohercynian synorogenic sandstone: implications for tectonic, 57, 173-188. (eds). Development in sedimentary provenance studies. Geological Society Special Publication
Fralick, P.W. and Kronberg, B.I. (1997) Geochemical Discrimination of Clastic Sedimentary Rock Sources. Sedimentary Geology, 113, 111-124. https://doi.org/10.1016/S0037-0738(97)00049-3
Gromet, L.P., Dymek, R.E., Haskin, L.A. and Korotev, R.L. (1984) The “North American Shale Composite”: Its Composition, Major and Trace Element Characteristics. Geochimica et Cosmochimica Acta, 48, 2469-2482. https://doi.org/10.1016/0016-7037(84)90298-9
Günther, M.A., Dulski, P., Lavreau, J., Lehmann, B., Möller, P., Pohl, W.L., (1989). The Kibara tin -granites: Hydrothermal alteration versus plate tectonic setting, IGCP 255. Newsletter 2, 21–27.
Herron, M.M., (1988). Geochemical classification of terrigenous sands and shales from core or log data. Journal of Sedimentary Petrology 58, 820–829.
Kanzira, H. (1989). Classification magmato-tectonique des granites du Rwanda. - IGCP n° 255 newsletters.
Klerkx, J., Li_egeois, J.P., Lavreau, J., Theunissen, K.,(1984). Granitoides kibariens précoces et tectonique tangentielle au Burundi : magmatisme bimodal lié à une distension crustale. In: Klerkx, J., Michot, J. (Eds.), African Geology, a Volume in Honour of L. Cahen. Mus_ee Royale d'Afrique Centrale, Tervuren, pp. 29e46.
Klerkx, J., Li_egeois, J.P., Lavreau, J., Claessens, W.,(1987). Crustal evolution of the northern Kibaran Belt, eastern and Central Africa. In: KrÖner, A. (Ed.), Proterozoic Lithospheric Evolution, Geodynamics Series (American Geophysics Union), vol. 17, pp. 217e233.
Ledent D., (1979), Données géochronologiques relatives aux granites Kibariens de type A (ou G1) et B (ou G2) du Shaba, du Rwanda, du Burundi et du Sud-ouest de l’Uganda. Mus. Roy. Afr. centr. Tervuren, Dépt. Géol. Min., Rapp. Ann., 1980,131-145
Lepersonne, J.,(1974). Carte géologique du Zaïre. Département des Mines, République du Zaïre. Musée royal de l'Afrique centrale.
Maynard JB, Valloni R, Yu HS (1982) Composition of modem deep sea sands L'om arc-related basins. In: Leggett, J.K. (Ed.), sedimentation and tectonics on modem and ancient plate margins. Geol., Soc. London spec. Publ 10:551–561
McLennan, S.M. (2001) Relationships between the Trace Element Composition of Sedimentary Rocks and Upper Continental Crust. Geochemistry, Geophysics, Geosystems, 2, 1021-1024. https://doi.org/10.1029/2000GC000109
Pearce M., Gorman, B.E., Birkett, T.C. (1975). The Relationship between Major Element Chemistry and Tectonic Environment of basic and intermediate Volcanic Rocks. Earth and Planetary Science Letters. 36(1), 121-132.
Pohl, W. (1987). Structural control of tin and tungsten mineralization in Rwanda, Africa. - Berg. Hüttenm. Monatsh.
Pohl, W. (1988). Post-orogenic events within and nearby the Kibara belt in Central Africa. - IGCP n° 255 newsletter.
Pohl, W. and Günther, M. (1989). Tectonic control and PIT conditions of the formation of Kibaran tin, tungsten

and gold deposit in central Africa. I.G.C.P., 255, Newsletter, 2, 101-105.
Pohl, W., Günther, M.A., (1991). The origin of Kibaran (late Mid-Proterozoic) tin, tungsten and gold quartz vein deposits in Central Africa: a fluid inclusion study. Miner. Deposita 26, 51e59.
Roser, B.P., Korsch, R.J., (1986). Determination of tectonic setting of sandstone-mudstone suites using SiO2 content and K2O/Na2O ratio. Journal of Geology 94, 635–650.
Roser, B.P., Korsch, R.J., 1988. Provenance signatures of sandstone–mudstone suite determined using discrimination function analysis of major-element data. Chemical Geology 67, 119–139.
Rudnick, R.L. and Gao, S. (2003) Composition of the Continental Crust. In: Rudnick, R.L., Ed., The Crust, Elsevier-Pergamon, Oxford, 1-64. https://doi.org/10.1016/B0-08-043751-6/03016-4
Rumvegeri, B. T. (1987). Le Précambrien de l'Ouest du lac Kivu (Zaïre) et sa place dans l'évolution géodynamique de l'Afrique centrale et orientale. Pétrologie et Tectonique. Thèse de doctorat ès Sci. Université de Lubumbashi, Fac. Sci, Dept. Geol., Vol.1.279p.
Sibson, R.H. and Scott, J. (1998) Stress/Fault Controls on the Containment and Release of Over pressured Fluids: Examples from Gold-Quartz Vein Systems in Juneau, Alaska; Victoria, Australia and Otago, New Zealand. Ore Geology Reviews, 13, 293-306. https://doi.org/10.1016/S0169-1368(97)00023-1
Sibson, R.H., Robert, F. and Poulsen, K.H. (1988) High Angle Reverse Faults Fluid Pressure Cycling and Mesothermal Gold-Quartz Deposits. Geology, 16, 551-555. https://doi.org/10.1130/0091-7613(1988)0162.3.CO;2
Sicke L., Ombeni B.J. (2017). Étude géologique, structural et gîtologique du secteur d'Imonga, secteur de Mulu, Maniema. B.Sc. dissertation, Université Libre de Grands Lacs,Bukavu,DR Congo.
Steenstra, B., (1967). Les pegmatites du Maniema et du Rwanda et les roches de transition entre les aplites et les pegmatites du Maniema. Miner. Deposita 2, 271e285.
Tack, L., Duchesne, J.C., Liégeois, J.P., Deblond, A. (1994) Two successive mantle-derived A-type granitoids in Burundi: Kibaran late-orogenic extentional collapse and lateral shear along the edge of Tanzanian craton. Precambrian Research.
Tack, L. Tack., M., Wingate., B., De Waele., J., Meert., E., Belousova., B., Griffin., A., Tahon., Fernandez-Alonso, L. (2010) The 1375 Ma "Kibaran event" in Central Africa: Prominent emplacement of bimodal magmatism under extensional regime. Precambrian Research. 180 (1-2), 63-84.
Taylor, S.R. and McLennan, S.M. (1985) The Continental Crust: Its Composition and Evolution. Blackwell Scientific Publication, Carlton, 312 p.
Tarney J. (1977) Petrology, Mineralogy and Geochemistry of the Falkland Plateau Basement Rocks, Site 300, Deep Sea Drilling Proect. Initial Report, 36, 893-921. https://doi.org/10.2973/dsdp.proc.36.123.1977
Taylor, S.R., McLennan, S.M., (1985). The Continental Crust: Its Composition and Evolution. Blackwell Scientific Publishers, Oxford.
Theunissen K., (1984), Les principaux traits de la tectonique Kibarienne au Burundi. UNESCO, Géol. for Economic Development. Newsletter, 2, 85-92.
Varlamoff, N., (1948). Gisements de cassitérite de la région de Kalima (Maniema, Congo belge). Ann. Soci. G_eol. Belg. 71, 194e237.
Varlamoff, N., (1950). Granites et minéralisation au Maniema (Congo belge). Ann. Soc. G_eol. Belg. 73, 111e163.
Varlamoff, N., (1954). Transitions entre les aplites et les pegmatites dans les zones de contact des massifs granitiques des concessions de Symetain à Kalima (Maniema, Congo belge). Ann. Soc. Geol. Belg. 77, 101e120.
Varlamoff, N., (1956). Transitions entre les pegmatites et les filons de quartz dans les massifs granitiques des régions stannifères du Maniema (Congo belge). Ann. Soc. Géol. Belg. 79, 385e403.
Villeneuve, M. (1977) Précambrien du Sud du lac Kivu. Etude stratigraphique, pétrographique et tectonique., p. 195.